Cell, Vol. 98, 475–485, August 20, 1999, Copyright ©1999 by Cell Press

Activation of Store-Operated Ca^{2+} Current in *Xenopus* Oocytes Requires SNAP-25 but Not a Diffusible Messenger

Yong Yao,* Antonio V. Ferrer-Montiel,†‖ Mauricio Montal,† and Roger Y. Tsien*‡§

*Department of Pharmacology
†Department of Biology
‡Howard Hughes Medical Institute
University of California, San Diego
La Jolla, California 92093-0647

Summary

Depletion of Ca^{2+} stores in *Xenopus* oocytes activated entry of Ca^{2+} across the plasma membrane, which was measured as a current I_{soc} in subsequently formed cell-attached patches. I_{soc} survived excision into inside-out configuration. If cell-attached patches were formed before store depletion, I_{soc} was activated outside but not inside the patches. I_{soc} was potentiated by microinjection of *Clostridium* C3 transferase, which inhibits Rho GTPase, whereas I_{soc} was inhibited by expression of wild-type or constitutively active Rho. Activation of I_{soc} was also inhibited by botulinum neurotoxin A and dominant-negative mutants of SNAP-25 but was unaffected by brefeldin A. These results suggest that oocyte I_{soc} is dependent not on aqueous diffusible messengers but on SNAP-25, probably via exocytosis of membrane channels or regulatory molecules.

Introduction

Ca^{2+} influx across the plasma membrane can be activated by depletion of intracellular Ca^{2+} stores in many nonexcitable cells, and it is important in activation of lymphocytes, exocytosis of mast cells, and other Ca^{2+}-dependent physiological events (for recent reviews, Berridge, 1995; Lewis and Cahalan, 1995; Favre et al., 1996; Parekh and Penner, 1997; Holda et al., 1998; Putney and McKay, 1999). The mechanism by which such "capacitative" Ca^{2+} entry is activated remains controversial. Major proposals include direct interaction ("conformational coupling") between proteins in organellar and plasma membranes (Berridge, 1995), diffusible messengers or calcium influx factors (CIFs) generated by store depletion (Parekh et al., 1993; Randriamampita and Tsien, 1993; Csutora et al., 1999), metabolites of phosphoinositides, phosphorylation cascades, heterotrimeric or small G proteins (Bird and Putney, 1993; Fasolato et al., 1993), and exocytotic insertion of vesicular channels into the plasma membrane. Previous arguments for exocytosis have included inhibition of capacitative Ca^{2+} entry by intracellular GTPγS (Bird and Putney, 1993; Fasolato et al., 1993), primaquine (Somasundaram et al., 1995), and the actin-depolymerizing drug cytochalasin D (Holda and Blatter, 1997). Each of these observations is controversial. Petersen and Berridge (1995) and Gregory and Barritt (1996) showed that the GTPγS inhibition of Ca^{2+} influx into oocytes could be prevented by staurosporine. They concluded that the GTPγS effect was mediated via stimulation of kinases. The effect of primaquine has been reinterpreted as direct inhibition of the Ca^{2+} influx channels (Gregory and Barritt, 1996). Cytochalasin D has no effect on capacitative Ca^{2+} entry in NIH3T3 cells, even though it blocks agonist-dependent Ca^{2+} release (Ribeiro et al., 1997). Furthermore, none of these pharmacological interventions is particularly diagnostic for exocytosis or takes advantage of our increased understanding of the macromolecules involved in membrane trafficking. Unfortunately, the channels that mediate capacitative Ca^{2+} influx have not yet been definitively identified at the molecular level.

This study began as a reexamination of the diffusible messenger hypothesis. Channels gated directly by diffusible messengers should be activatable in cell-attached configuration, lost in excised patches, and reactivated upon cramming those inside-out patches into the cytosol of preactivated cells, as first shown for cyclic-nucleotide-gated cation channels by Kramer (1990). Parekh et al. (1993) reported analogous behavior for capacitative Ca^{2+} entry into *Xenopus* oocytes, though Ca^{2+} entry was not directly monitored but only surmised from currents of uncertain ionic basis. Recently, we showed that store-operated, capacitative Ca^{2+} currents (I_{SOC}) into whole oocytes could be directly measured by buffering cytosolic Ca^{2+} to prevent secondary currents, perfusing extracellularly with isotonic Ca^{2+} and Mg^{2+} alternately, and quantitating the difference in currents (Yao and Tsien, 1997). We have now extended this protocol to cell-attached and excised patches, hoping to solidify the evidence of Parekh et al. (1993) for a diffusible messenger. In addition, inside-out patches would be useful online detectors for the diffusible messenger(s) and would facilitate chromatographic purification and chemical identification. To our surprise, our patch-clamp findings (see Results) argued against simple mechanisms involving reversible binding of diffusible messengers.

We therefore sought experimental approaches that would be more diagnostic for an exocytotic coupling mechanism than those employed previously. We tried modulation of the small G protein Rho, because *Clostridium botulinum* C3 transferase, which specifically inactivates Rho through ADP ribosylation of Rho at Asn-41, was shown to increase insertion of the insulin-sensitive glucose transporter GLUT4 into the plasma membrane in 3T3-L1 adipocytes (Van den Berghe et al., 1996). C3 transferase also increases membrane capacitance and externalization of sodium pumps in *Xenopus* oocytes, possibly by blockade of constitutive endocytosis (Schmalzing et al., 1995).

We tested botulinum neurotoxins (BoNTs), a group of zinc endoproteases produced by bacteria of the genus *Clostridium*, because they display specific activity for a triad of protein components of the exocytic apparatus:

§To whom correspondence should be addressed (e-mail: rtsien@ucsd.edu).
‖Present address: Centro de Biologia Molecular y Celular, Universidad Miguel Hernández, C/ Monóvar s/n, 03206 Elche, Spain.

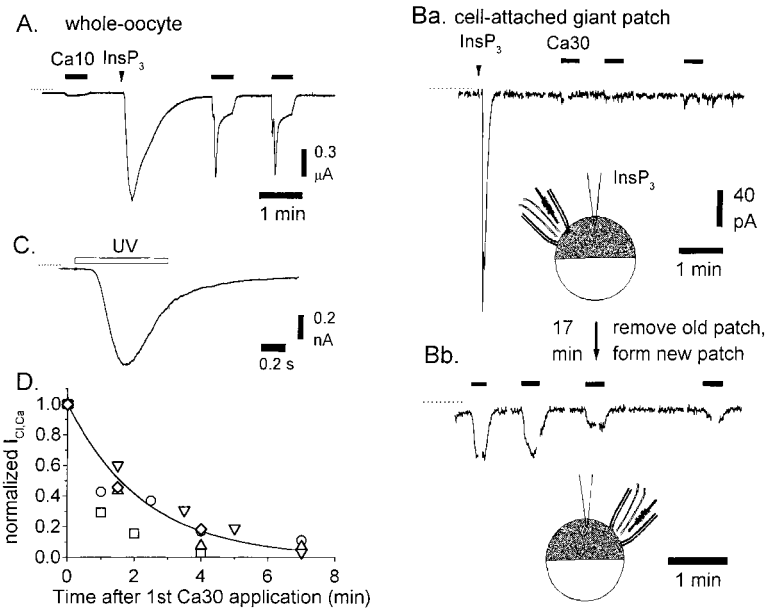

Figure 1. Blockade of Activation of Store-Operated Ca^{2+} Influx by GΩ Sealing Procedure

(A) Ca^{2+} release activated Ca^{2+} influx in oocyte recorded with two-electrode voltage clamp. Ca^{2+} influx was monitored by switching bath from Mg70 to Ca10 where indicated by heavy bars. Dotted lines in this and subsequent panels indicate zero current levels.

(Ba) Ca^{2+} release failed to activate Ca^{2+} influx in preformed cell-attached giant patch. Solution inside patch pipette was alternately changed between Mg70 and Ca30 Ringer.

(Bb) A new cell-attached giant-patch recording was made about 17 min after $InsP_3$ injection from the same oocyte. Note that the Ca^{2+} influx was recorded now in the patch formed after activation of the capacitative Ca^{2+} influx. $InsP_3$ (2 mM of 25 nl) was injected in both recordings from whole oocyte and patch as indicated by arrow heads in (A) and (B). Voltage ramps were repetitively applied during the patch recording to monitor the I-V curve. The corresponding transient currents have been blanked for clarity.

(C) $I_{Cl,Ca}$ was elicited by uncaging caged $InsP_3$ in a cell-attached giant patch. Oocyte had been loaded with 30 nl of 10 mM caged $InsP_3$.

(D) Deactivation of store-operated Ca^{2+} influx in cell-attached giant patches from $InsP_3$-loaded oocytes. Ca^{2+} influx–induced $I_{Cl,Ca}$ was measured at $V_m \approx +50$ mV and normalized to the first current amplitude. Data from five patch recordings were plotted against the time after first exposure to Ca30, among which three were made subsequently from a same oocyte. The smooth curve was a single exponential fit with a decay time constant of around 2 min.

a vesicle-associated membrane protein (VAMP or synaptobrevin), and two plasma membrane–attached proteins, SNAP-25 and syntaxin (Montecucco and Schiavo, 1995). BoNT B, D, F, and G recognize and cleave VAMP specifically. BoNT A and E cleave SNAP-25 specifically. BoNT C1 cleaves syntaxin. Binding of VAMP to syntaxin is facilitated by SNAP-25, which leads finally to fusion of vesicles with plasma membrane (Calakos and Scheller, 1996). BoNTs are widely used to block regulated exocytosis in secretory cells. Finally, dominant-negative mutants of SNAP-25 provided a molecularly independent confirmation of the BoNT A results. The combined results argue that SNAP-25 and presumably membrane trafficking play essential roles in the activation of oocyte I_{SOC}.

Results

Prior Gigaseal Formation Prevents Store Depletion from Activating Ca^{2+} Entry inside but Not outside the Patch

As well-established in two-electrode voltage clamp recording (Yao and Tsien, 1997), Ca^{2+} release due to injection of $InsP_3$ invariably led to Ca^{2+} influx, which caused a Ca^{2+}-activated Cl^- current $I_{Cl,Ca}$ whenever external Ca^{2+} was present (solid horizontal bars in Figure 1A). In these cells, we did not inject Ca^{2+} chelators to buffer cytosolic Ca^{2+}, so that $I_{Cl,Ca}$ could be a maximally sensitive monitor of Ca^{2+} entry. In contrast, when currents were recorded in cell-attached giant patches, injection of a saturating dose of $InsP_3$ activated only a transient $I_{Cl,Ca}$ mediated by Ca^{2+} release, but not Ca^{2+} influx (Figure 1Ba, typical of 10 of 11 patches). Interestingly, Ca^{2+} influx could be recorded subsequently in cell-attached patches at different spots from the same oocyte (Figure 1Bb). This indicated that prior formation of a gigaohm seal blocked the coupling mechanism between store depletion and Ca^{2+} entry within the pipette, whereas Ca^{2+} entry outside the pipette activated normally.

In a separate group of experiments, TPEN (Hofer et al., 1998) was used as an independent activator to confirm the above curious finding. In two-electrode voltage clamp recordings from whole oocytes, application of 5 mM TPEN induced Ca^{2+} influx-mediated $I_{Cl,Ca}$ of 200 to 600 nA in 10 mM extracellular Ca^{2+}. This much whole-cell current should give 31–94 pA $I_{Cl,Ca}$ in giant patches of 30 μm diameter given the ratio of giant-patch to whole-cell areas, 1/6400. However, there was no detectable Ca^{2+} influx-mediated $I_{Cl,Ca}$ in 12 of 14 cell-attached giant patches under similar stimuli measured with pipettes filled with 10 mM Ca^{2+}. In the remaining two patches, the $I_{Cl,Ca}$ mediated by Ca^{2+} influx was only −3 and −5 pA, approximately one order of magnitude less than predicted from the ratio of membrane areas. This result confirmed that most cell-attached giant patches did not respond to stimuli that normally activate store-operated Ca^{2+} influx.

The plasma membrane in cell-attached patches was visibly somewhat invaginated into the patch pipette, as is common in patch clamping (Sokabe and Sachs, 1990). To estimate the diffusional distance between the stores and plasma membrane patch, oocytes were loaded with caged $InsP_3$, and the latency of $I_{Cl,Ca}$ in giant patches after UV flash was measured (Figure 1C). This latency resulted mainly from the delay time of $InsP_3$-evoked Ca^{2+} release plus time for Ca^{2+} to diffuse from the stores to plasma membrane (Parker and Ivorra, 1993). Hot spots of $InsP_3$-evoked Ca^{2+} release are normally located about 5 μm deep under the plasma membrane in oocytes (Yao et al., 1995). This distance (d) corresponds well with 30

ms latency (t) between the Ca^{2+} fluorescence signal and $I_{Cl,Ca}$, a Ca^{2+} diffusion coefficient (D) of 140 $\mu m^2 s^{-1}$, and the equation $d^2 = 6Dt$ (Allbritton et al., 1992; Parker and Ivorra, 1993). The latency of $I_{Cl,Ca}$ in giant patches after UV uncaging of $InsP_3$ was 210 ± 30 ms (n = 3). This 7-fold increase in latency corresponds to a mean effective distance of 13 μm between stores and plasma membrane. The modest increase in distance from 5 to 13 μm should not be enough to prevent diffusion of a small molecule activator.

Maintenance of Store-Operated Ca^{2+} Influx in Whole Cells, Cell-Attached, and Excised Patches

When oocytes were injected with a saturating dose of $InsP_3$, about 0.2 mM, the Ca^{2+} influx assayed by two-electrode voltage clamp recording of $I_{Cl,Ca}$ or whole-cell recording of I_{SOC} lasted >0.5 hr. However, once a patch was formed on an activated cell, $I_{Cl,Ca}$ measured from the enclosed patch as the difference of currents with 30 mM versus 0 Ca^{2+} in the pipette declined with a time constant of about 2 min. Figure 1Bb shows one example, while Figure 1D shows the pooled data from five recordings. This decay probably represented unmasking of deactivation after gigaseal formation had blocked any further activation within the patch.

The above experiments were performed with $I_{Cl,Ca}$ as the most sensitive index of Ca^{2+} entry to maximize its likelihood of detection within the patch. We were also able to detect the much smaller Ca^{2+} current itself, I_{SOC}, in similar patches if cytosolic Ca^{2+} was well buffered by EGTA injection and store depletion preceded gigaseal formation (Figure 2A). The intrapipette solution was perfused alternately with 70 mM Mg^{2+} (Mg70) and 70 mM Ca^{2+} (Ca70), and the difference of currents $I_{Ca70} - I_{Mg70}$ was taken as I_{SOC} (Yao and Tsien, 1997). In average, I_{SOC} measured in cell-attached giant membrane patches was −22.1 ± 2.7 pA (n = 32) in oocytes depleted with ionomycin, versus −3.6 ± 0.5 pA (n = 13) from control oocytes. The amplitude of I_{SOC} in preactivated patches corresponded well with that predicted from 1/6400 of the area of a whole oocyte. Ramp current traces a and b were obtained, respectively, in Mg70 and Ca70 (Figure 2Ba) and showed an I-V relation similar to that measured in whole oocytes with two-electrode voltage clamp (Yao and Tsien, 1997).

After excision of the patch into a mock intracellular Ringer with 0 Ca^{2+} and 5 mM EGTA, I_{SOC} was constant or increased with time (Figure 2A) in 12 out of 15 patches, unlike the rapid decay of Ca^{2+} entry in patches left attached to unbuffered cells (Figures 1Bb and 1D). In the other three patches, I_{SOC}-like current decayed to baseline after a few minutes. On average, this inward current was sustained for at least 4 min after patch excision (Figure 2C). In our longest recording, lasting 8 min after excision, I_{SOC} was sustained throughout. I_{SOC} in excised patches was larger and noisier at negative membrane potentials but otherwise had much the same I-V relationship (Figure 2Bb) as before excision. To verify that the former cytosolic face of the patch was truly exposed to the bath, the external solution was briefly switched to a buffer with 0.2 μM [Ca^{2+}], which activated $I_{Cl,Ca}$ as expected (Figure 2A shaded bar and I-V relation in Figure 2Bc). In oocytes without ionomycin incubation, the residual currents measured by the usual protocol ($I_{Ca70} - I_{Mg70}$) were small and not significantly affected by excision, 4.7 ± 0.7 pA (n = 6) before versus 4.8 ± 1.0 pA (n = 6) after excision.

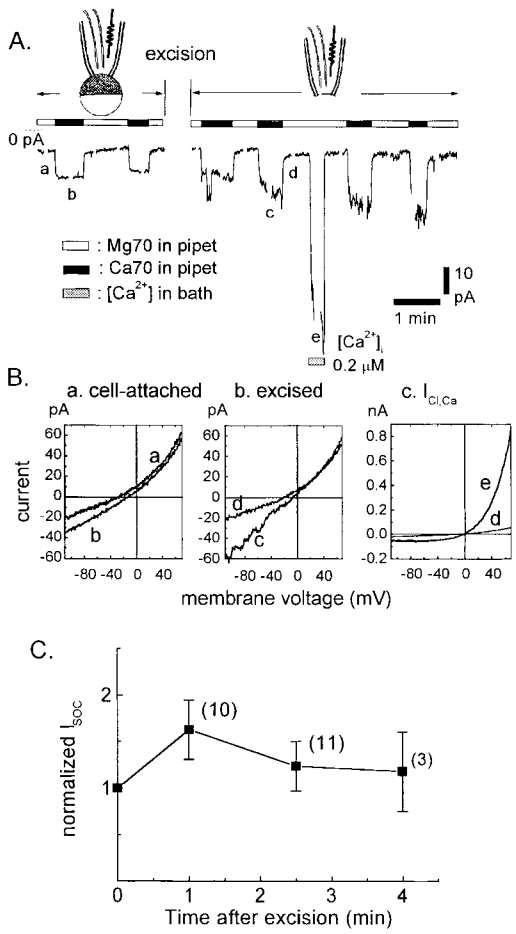

Figure 2. Survival of I_{SOC} in Inside-Out Giant Patches

(A) Store-operated Ca^{2+} current in cell-attached and inside-out giant patch. Oocyte was treated with ionomycin and injected with EGTA before patching. Pipette solution was alternately perfused with Mg70 (indicated with open bar) and Ca70 (solid bar). Voltage ramps were applied periodically to obtain the I-V curves shown in (B). The evoked current transients have been blanked for clarity.

(B) I-V curves were obtained respectively in Mg70 and Ca70 in cell-attached patch (measured at time a and b in [A]; shown in [Ba]), and in inside-out patch (c and d in [Bb]). $I_{Cl,Ca}$ was activated in excised patch by a transient increase of bath [Ca^{2+}] (e).

(C) Average of normalized I_{SOC}-like current after patch excision. The number in parentheses indicates number of patch recordings made.

Thus, seal formation on the outside of the plasma membrane inhibited activation of new I_{SOC} inside the patch but allowed preactivated I_{SOC} to continue; maintenance of such I_{SOC} did not require presence of cytosolic substances and was actually enhanced by excision. These results suggest that activation of I_{SOC} is rather localized, sensitive to membrane deformation, and unlikely to result from simple diffusion of an activator molecule. Furthermore, activation and deactivation seem to be separate processes not linked by a simple equilibrium, because different orders of manipulation can give very different results.

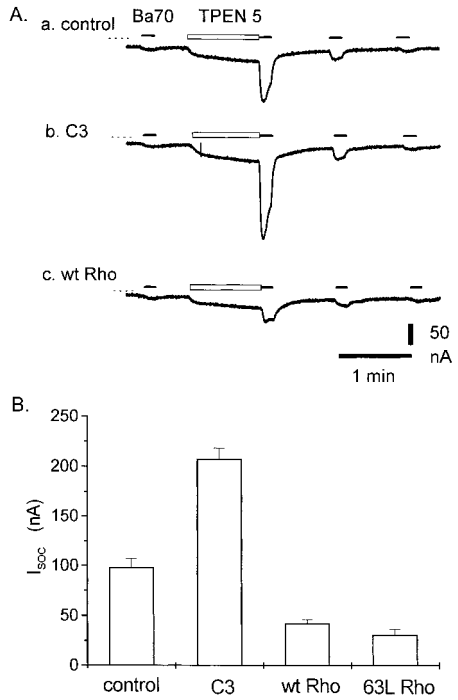

Figure 3. I_{SOC} Was Potentiated by Injection of C3 Transferase and Inhibited by Expression of Rho A

(A) I_{SOC} was induced by TPEN 5 mM in bath (open bars) and monitored by switching from Mg70 to Ba70 (solid bars). I_{SOC} evoked by TPEN was rapidly reversible. Recordings were made, respectively, in native oocyte (Aa), oocyte 1 hr after injection of C3 transferase 0.4 μM (Ab), and oocyte 6 hr after injection of 20 ng Rho A cRNA (Ac).
(B) Summary of effects on I_{SOC} of microinjected C3 transferase, expression of wild-type Rho A, and its constitutively active mutant 63L.

Regulation of Store-Operated Ca^{2+} Influx by Rho A

To examine whether the store-operated Ca^{2+} influx was affected by Rho, C3 transferase was microinjected into oocytes. In recordings illustrated in Figure 3A, Ba^{2+} current was measured to quantitate effects of C3 and Rho. Injection of Ca^{2+} chelators was omitted because activation of $I_{Cl,Ca}$ by Ba^{2+} was negligible. I_{SOC} induced by 5 mM TPEN was 98 ± 9 nA (n = 9) in control oocytes and 207 ± 11 nA (n = 7) in oocytes measured about 1–2 hr after injection of C3 (3 ng/oocyte, or 120 nM assuming uniform distribution in 1 μl cytosol), an increase of 2.1-fold ($p < 0.01$). In complementary experiments, Rho A, its constitutively active mutant (63L), and dominant-negative mutant (19N) were expressed in oocytes by injection of 20 ng of their respective cRNAs about 5 hr before recordings started. I_{SOC} was 42 ± 4 nA (n = 4) in oocytes expressed with wild-type Rho and 31 ± 6 (n = 6) with constitutively active mutant (63L), corresponding to 57% ($p < 0.01$) and 68% ($p < 0.01$) inhibition, respectively (Figure 3B). I_{SOC} remained unchanged in oocytes expressing dominant-negative mutant 19N Rho A, suggesting a large pool of endogenous Rho A existed to maintain basal activity. Injection of C3 also induced an increase of membrane capacitance. Membrane capacitance increased by about 41% in 2 hr after injection of C3 (3 ng/oocyte) (n = 7, $p < 0.01$). In contrast, no significant decrease in membrane capacitance was found to accompany inhibition of I_{SOC} in oocytes expressed with wt Rho (n = 4) and 63 L Rho (n = 6). Amplitude of I_{SOC} activated by 5 mM TPEN in the above experiments was about half of the maximum. Maximal I_{SOC} induced by a saturating dose of ionomycin (10 μM) was also enhanced about 46% (n = 9, $p < 0.01$) by C3 transferase. Oocytes from five of six animals showed a similar extent of potentiation by C3 transferase but not in the remaining one frog. This suggested that Rho played a modulatory rather than an indispensable role in activation of I_{SOC}.

Because one of the many effects of active Rho is to promote assembly of actin-myosin filaments (stress fibers), we examined whether the potentiation of I_{SOC} by C3 might simply result from the disruption of the actin-myosin assembly. Oocytes were treated with cytochalasin D (20 μg/ml) for 17 hr, at which time oocytes appeared mottled as an indication of actin depolymerization and had relative low input resistance. I_{SOC} was 118 ± 14 nA (n = 7) in control oocytes and 93 ± 17 nA (n = 7) in oocytes treated with cytochalasin D. Thus, destruction of the actin cytoskeleton by cytochalasin D slightly reduced I_{SOC}, probably by nonspecific mechanisms rather than mimicking C3 transferase, which greatly potentiated I_{SOC}. We also tried 5 μM jasplakinolide, which solidifies the actin cytoskeleton (Shurety et al., 1998). I_{SOC} was reduced from its control value of 87 ± 9.5 nA (n = 4) to 64 ± 3 nA (n = 6) during drug exposures of 0.5 or 2 hr, which were equivalent. This small reduction was significant at the p = 0.026 level and was in the same direction as, but much weaker than, the complete inhibition by 3 μM jasplakinolide of store-operated Ca^{2+} entry in cultured mammalian cells (Patterson et al., 1999 [this issue of *Cell*]).

BoNT A Inhibits Activation of Store-Operated Ca^{2+} Influx

Preinjection with 100 nM BoNT A reduced I_{SOC} by about 50% (Figures 4Aa and 4Ba) without any effect on the inward rectification or the leak current, as shown by the I-V curves in Mg70 and Ca70 (Figures 4Ab and 4Bb). BoNT A also reduced Ca^{2+} influx-dependent $I_{Cl,Ca}$ induced by ionomycin, $InsP_3$, and TPEN in 10 mM Ca_o by 89% (n = 11, $p < 0.01$), 86% (n = 4, $p < 0.01$), and 86% (n = 6, $p < 0.01$), respectively (data not shown). The more dramatic reduction in the $I_{Cl,Ca}$ compared to I_{SOC} probably reflects the nonlinear relation of the former with I_{SOC} (Yao and Tsien, 1997). No significant change in the resting potential, input resistance, and membrane capacitance were found by BoNT A. Also, BoNT A did not alter the $I_{Cl,Ca}$ transients elicited by ionomycin, $InsP_3$, or TPEN in calcium-free medium, showing that the release of Ca^{2+} from stores and the properties of $I_{Cl,Ca}$ were unaltered.

The kinetics of BoNT A action are shown in Figure 4C. The inhibition developed with an apparent single exponential time constant of 1.1 hr and reached maximum about 4 hr after BoNT A administration. I_{SOC} was 141 ± 9 nA (n = 9) in control oocytes and 72 ± 3 nA (n = 7, $p < 0.01$) in oocytes about 4 hr after injection of BoNT A. The inhibition was long-lasting and still apparent after 2 days. In a separate double-blind experiment, various doses of BoNT A were injected into oocytes. I_{SOC} was measured 4 to 7 hr after injection of 20 nl BoNT A of different concentrations. The inhibition of

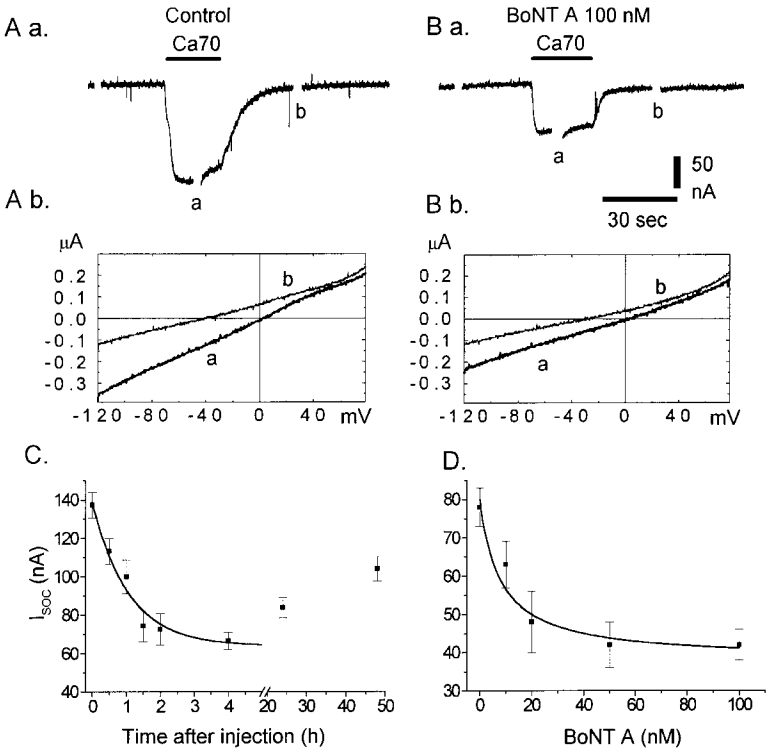

Figure 4. Inhibition of I_{SOC} by BoNT A

I_{SOC} was activated by 5 μM ionomycin followed by injection of EGTA to a final internal concentration of about 10 mM and was recorded by switching from Mg70 to Ca70 (solid bars) in a control oocyte (Aa) and an oocyte injected 4 hr earlier with 100 nM BoNT A (Ba). (Ab and Bb) The I-V relations obtained in Ca70 (a) and Mg70 (b). (C) Kinetics of BoNT A action. I_{SOC} was activated as above at different times after injection of BoNT A 100 nM. The smooth curve was the best fit to a single exponential decay with a time constant of 1.1 hr. Each data point was from more than three oocytes. (D) Dose dependence of BoNT A action. Oocytes were injected with different concentrations of BoNT A as indicated. Recordings were made 4 to 7 hr after the injections. Each data point was the average of more than four oocytes. Smooth curve was a fit to equation $(I - I_{min})/(I_{max} - I_{min}) = K_i/(K_i + [BoNT])$, with I_{max} = 80 nA, I_{min} = 38 nA, K_i = 8 nM.

I_{SOC} was found to be dose dependent on BoNT A with an apparent $K_i \approx 8$ nM (Figure 4D).

In contrast to BoNT A, BoNT B, E, and tetanus toxin had no significant effects on I_{SOC} measured about 6–8 hr after injection to final concentrations of 200 nM each. I_{SOC} was 93 ± 4 nA (n = 6) in control oocytes versus 74 ± 4 nA (n = 4), 78 ± 5 (n = 5), and 73 ± 8 (n = 6) in oocytes injected with BoNT B, E, and tetanus toxin, respectively. Unfortunately, we cannot yet test biochemically whether our toxin samples could cleave *Xenopus* oocyte SNAREs because the latter have not yet been cloned, and the antibodies we had against the mammalian proteins did not recognize their oocyte counterparts.

Blockade of I_{soc} by Dominant-Negative Mutants of SNAP-25

Because the usual target of BoNT A is SNAP-25, we examined whether I_{SOC} activation could be similarly inhibited by dominant-negative mutants of SNAP-25. It was shown in yeast that sec9-Δ17, a C-terminal truncation of a SNAP-25 homolog, was a dominant-negative mutant (Rossi et al., 1997). According to sequence alignment (Weimbs et al., 1998) supported recently by crystal structure data (Sutton et al., 1998), yeast sec9-Δ17 corresponds to deletion of C-terminal 20 amino acids of mouse SNAP-25 (Δ20). BoNT A cleavage of mammalian SNAP-25 causes C-terminal truncation of nine amino acids (Δ9). Therefore, we made a series of C-terminal truncated SNAP-25 mutants spanning between Δ9 and Δ20 to examine whether they would have any inhibitory action on I_{SOC}. A truncated mutant SNAP-25 Δ41 was also made that corresponded to sec9-Δ38, which did not show dominant-negative effects in yeast (Rossi et al., 1997). The SNAP-25 mutants were expressed in oocytes by injection of their cRNA. I_{SOC} activated by TPEN was measured in oocytes about 14 hr after injection of 3 ng cRNA per oocyte of full-length, Δ9, Δ20, or Δ41, respectively (Figure 5). TPEN 5 mM induced about 100 nA I_{SOC} in uninjected oocytes and oocytes expressing full-length (Figure 5Aa) and Δ41 SNAP-25 (Figure 5Ac), but no I_{SOC} in oocytes expressing Δ20 (Figure 5Ab). I_{SOC} activation was inhibited by about half in oocytes expressing Δ9 cRNA. I_{SOC} activated by ionomycin was similarly inhibited by the expression of dominant-negative SNAP-25 mutants (Figure 5B). Oocytes were injected with 1 ng cRNA of each mutant per cell and recorded in 15 hr after the injection. I_{SOC} activated by 10 μM ionomycin was not affected by expression of full-length SNAP-25, but almost completely abolished by expression of Δ11, Δ14, Δ17, and Δ20 mutants. The inhibitory kinetics could be speeded up by injection of larger amounts of cRNA to express more proteins in shorter time. Thus, after injection of 30 ng of SNAP-25-Δ20, inhibition of I_{SOC} activated by ionomycin started in 2 hr and reached maximum within 4 hr after the injection (Figure 5C). While I_{SOC} was totally abolished, $I_{Cl,Ca}$ activated by ionomycin in calcium-free medium was unaffected in peak amplitude and more prolonged in oocytes expressing the dominant-negative mutant of SNAP-25, showing that inhibition of I_{SOC} was not due to any interference with Ca^{2+} release from stores. Furthermore, $I_{Cl,Ca}$ elicited by membrane depolarization (Barish, 1983) was not reduced by the dominant-negative mutants of SNAP-25. The effect of SNAP-25 on membrane turnover was assessed by capacitance measurements. A reduction of about 50% of total membrane capacitance was observed in oocytes injected with SNAP-25-Δ20 (189 ± 3 nF in control oocytes versus 96 ± 11 nF in SNAP-25-Δ20-expressed oocytes). This confirmed that the dominant-negative mutants of SNAP-25 were affecting plasma membrane turnover.

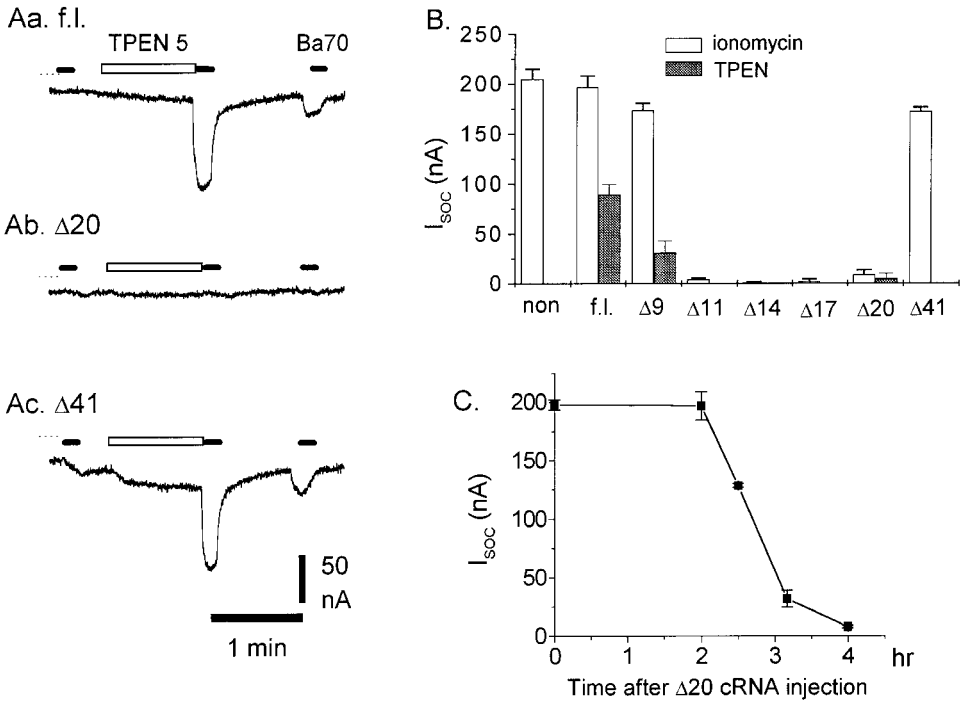

Figure 5. Prevention of I_{SOC} by C-Terminal Truncated Mutants of SNAP-25

(A) Activation of I_{SOC} by TPEN was not affected in oocytes expressing full-length (f.l.) SNAP-25 (Aa) and SNAP-25-Δ41 (Ac), but it was completely absent in oocytes expressing Δ20.

(B) Summary of inhibition of I_{SOC} by expressing SNAP-25 mutants. Activation of I_{SOC} by ionomycin (open columns) was totally abolished by expression of SNAP-25-Δ11, Δ14, Δ17, and Δ20 4 hr after injection of 30 ng cRNA, respectively. Activation of I_{SOC} by TPEN (filled columns) was inhibited by about half by expressing SNAP-25-Δ9 and was almost totally blocked by expressing Δ20 in 17 hr after injection of 3 ng cRNA each.

(C) Kinetics of I_{SOC} inhibition by expression of SNAP-25-Δ20. I_{SOC} was activated by ionomycin and measured at various times after the injection of 30 ng cRNA.

Activation of I_{SOC} Is Not Inhibited by Brefeldin A

To distinguish whether inhibition of I_{SOC} by BoNT A and dominant-negative mutants of SNAP-25 was mediated by interference with constitutive versus regulated exocytosis, we compared the effects of brefeldin A (BFA) with those of BoNT A and SNAP-25 Δ20. BFA blocks constitutive exocytosis by inhibiting protein exit from Golgi apparatus, which possibly results from BFA inhibition of guanine nucleotide exchange for ARF, a small G protein that is involved in coatomer-mediated vesicle budding from ER (Peyroche et al., 1999). Wild-type amiloride-sensitive epithelial sodium current (ENaC) expressed in *Xenopus* oocytes is inhibited by 5 μM BFA with a time constant of 3.6 hr due to blockade of constitutive insertion of ENaC channels while clathrin-mediated endocytosis remains active (Shimkets et al., 1997). We confirmed such downregulation of ENaC in oocytes by BFA as a positive control for BFA efficacy. I_{ENaC} was reduced by about 86% ($p < 10^{-10}$) by incubation of oocytes with BFA 5 μM for 7 hr. I_{SOC}, however, remained unchanged after incubation of oocytes in 5 μM BFA for 7 to 20 hr in the same batch of oocytes (Figure 6). In complete contrast to BFA, BoNT A inhibited I_{SOC} ($p < 10^{-28}$) but not I_{ENaC}. A dominant-negative SNAP-25 mutant slightly inhibited I_{ENaC} ($p = 0.014$), but to a much lesser extent than did BFA (Figure 6). In addition to the exogenous Na^+ channels, the endogenous voltage-operated Ca^{2+} channels and Ca^{2+}-activated Cl^- channels were not reduced by BoNT A and SNAP-25-Δ20 but were inhibited by BFA, though the BFA block was statistically significant only at the $p = 0.06$ level (Figure 6). These results indicated that blockade by BFA of constitutive traffic to the plasma membrane for up to 24 hr did not reduce the cells' ability to activate I_{SOC}, and inhibition of I_{SOC} by BoNT A and SNAP-25 mutants did not result from disruption of constitutive trafficking.

Discussion

Activation of the Store-Operated Ca^{2+} Current Is a Local Process that Can Show Hysteresis

Our patch-clamp experiments showed that store-operated Ca^{2+} entry was highly localizable, required store depletion to precede patch isolation, and yet survived patch excision. Thus, depletion of Ca^{2+} stores could activate Ca^{2+} influx outside but not inside a preformed gigaseal onto a 30 μm diameter patch pipette (Figures 1A and 1B). Therefore, the ability of store depletion to trigger Ca^{2+} current within the patch was disrupted by some aspect of seal formation, such as the visible invagination of the plasma membrane into the lumen of the pipette. Meanwhile, the $InsP_3$-induced increase in cytosolic [Ca^{2+}] was still able to activate $I_{Cl,Ca}$ within the cell-attached patch with slightly greater latency than normal (Figure 1C). This finding showed that Ca^{2+} was still able to diffuse from the internal stores to the plasma membrane inside the gigaseal, though the mean diffusion distance had apparently been increased from the normal

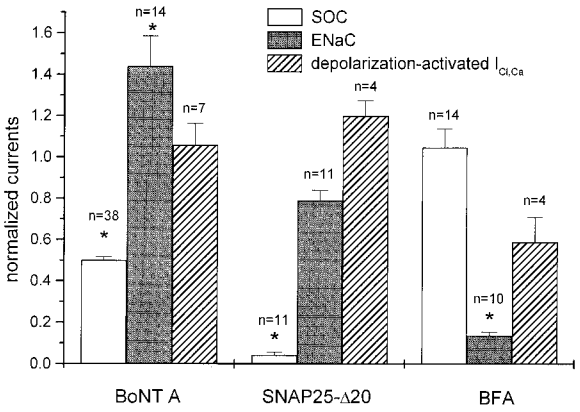

Figure 6. Comparison of Effects on I_{SOC}, I_{ENaC}, and Depolarization-Activated $I_{Cl,Ca}$ by BoNT A, SNAP-25-Δ20, and BFA

All current values measured were normalized to mean values of control groups of the same donor. The normalized currents from separate donors were averaged for statistical analysis. Groups significantly different ($p < 0.01$) from control are marked with an asterisk. Number of oocytes measured in each group is indicated on the column. I_{SOC} was activated by ionomycin and measured in Ba70. I_{ENaC} was measured in calcium-free Ringer at holding $V_m = -30$ mV as the difference in currents before and after 1 μM amiloride. Peak values of depolarization-activated $I_{Cl,Ca}$ were measured by stepping V_m to +40 mV in Ca10. It represents endogenous voltage-gated Ca^{2+} channel activity evoking $I_{Cl,Ca}$ (Barish, 1983). BoNT A was injected into oocytes to a 100–200 nM final concentration, waiting for 4 to 7 hr before recording. SNAP-25-Δ20 cRNA (30 ng) was injected into oocytes to allow protein expression for 4–6 hr. Incubations with 5 μM BFA lasted 5–20 hr before recording.

5 μm to 13 μm. Once Ca^{2+} influx was activated in the absence of or outside a gigaseal, it was readily detectable in a new cell-attached patch, showing that patch formation only obstructed initial activation rather than maintenance of the influx. Furthermore, I_{SOC} survived without diminution for minutes after excision of the patch into the inside-out configuration (Figure 2). Although one of us helped launch the idea of a diffusible CIF (Randriamampita and Tsien, 1993), we must admit that these findings argue against mediation by a CIF freely diffusible through the cytosol, because such a factor should have easily reached the plasma membrane inside the gigaseal but should have washed out immediately after excision of the patch. In a "conformational coupling" hypothesis, one would need to postulate that the protein–protein contact between the stores and plasma membrane would be easily disrupted or prevented before store depletion, but it would become robust enough after I_{SOC} activation to survive invagination and excision of the patch. In an exocytosis model, one would assume that exocytosis is locally prevented by bulging of the plasma membrane into the gigaseal. Indeed, exocytosis in mast cells is reported to be reversibly blocked by inflating the plasma membrane (Solsona et al., 1998). Whatever the model, the gigaseal results show that activation of Ca^{2+} influx can vary over distances of only a few microns, even more spatially confined than those of Petersen and Berridge (1996) or Jaconi et al. (1997), where localization was reported over distances of hundreds of microns.

These results would seem to conflict with a previous report (Figure 2, Parekh et al., 1993) in which a depletion-activated current in cell-attached patches was immediately quenched by excision from the oocyte and could be reactivated by cramming back into a stimulated cell. This current had a linear I-V curve with a reversal potential of −30 mV, was recorded in the presence of niflumic acid to block $I_{Cl,Ca}$, and had amplitudes of 10–20 pA with pipettes of ordinary micron diameters. I_{SOC} was characterized in recent two-electrode voltage clamp recording studies (Hartzell, 1996; Yao and Tsien, 1997), in which Ca^{2+} chelators instead of niflumic acid were used to abolish $I_{Cl,Ca}$ because niflumic acid was found to inhibit I_{SOC}. As expected for a highly Ca^{2+}-selective current, I_{SOC} has an inwardly rectifying I-V curve with a reversal potential $> +40$ mV. Giant-patch recording (Hilgemann, 1995) with 30 μm diameter pipettes and intrapipette perfusion was required to increase detection sensitivity and to record ~10 pA of I_{SOC} directly as the difference in currents between 70 and 0 mM extracellular Ca^{2+}. Therefore, the current that was quenched by excision and restored by cramming in the experiment of Parekh et al. (1993) was dominated by components other than Ca^{2+} influx.

Mechanisms of Rho A Action on I_{SOC}

Up- and downregulation of RhoA, by expression of excess Rho A or injection of *Clostridium* C3 transferase, respectively, decreased and increased the amplitude of I_{SOC} (Figure 3). Rho A is known to regulate many cell events, including cytoskeletal rearrangement and membrane trafficking (Van Aelst and D'Souza-Schorey, 1997; Hall, 1998). Because RhoA may affect both constitutive and regulated membrane trafficking, our results with C3 and RhoA provide only general evidence for the importance of trafficking in modulating capacitative Ca^{2+} entry.

Mechanisms of Action of Botulinum Neurotoxin A and SNAP-25

In this study, I_{SOC} was found to be inhibited by about 50% by BoNT A (Figures 4 and 6). This inhibition was relatively specific as endogenous $I_{Cl,Ca}$, voltage-gated Ca^{2+} current, and transfected epithelial Na^+ channels were not reduced. The time course and potency of the inhibitory action on I_{SOC} by BoNT A were similar to that described in blockade of neurotransmission of *Aplysia* synapses (Rossetto et al., 1994). Recently BoNTs have also been shown to block insulin-stimulated translocation of GLUT4 in adipocytes (Cheatham et al., 1996). The maximum inhibition of insulin-stimulated glucose uptake was 43%–51% (Tamori et al., 1996; Chen et al., 1997), quite similar to the maximal reduction of I_{SOC} in our experiments. Likewise BoNT A causes only a partial block and slowing of catecholamine release from chromaffin cells (Xu et al., 1998).

The complete inhibition of I_{SOC} by dominant-negative mutants of SNAP-25 and the biphasic length dependence of the effective truncations strongly complement the evidence from BoNT A for a crucial role for a SNAP-25 homolog in oocytes. The length dependence fits well with multiple studies showing the critical importance of the region corresponding to 9 to 26 residues from the C terminus of mammalian SNAP-25 for exocytosis and its triggering by calcium sensors (Gutierrez et al., 1995;

Rossi et al., 1997; Ferrer-Montiel et al., 1998; Huang et al., 1998; Xu et al., 1998). The partial inhibition by the Δ9 truncation fits well with the similarly partial inhibition by BoNT A, which should cut SNAP-25 at the corresponding location. The inhibition of I_{SOC} is not explainable by general interference with constitutive insertion of channels into the plasma membrane, because currents through Ca^{2+}-activated Cl^- channels, voltage-gated Ca^{2+} channels, or transfected epithelial Na^+ currents remained undiminished (Figure 6). Conversely, constitutive insertion, for example of epithelial Na^+ channels, can be inhibited by brefeldin A without any effect on I_{SOC} (Figure 6). Therefore, SNAP-25 and, presumably, regulated exocytosis are important in the process for activating I_{SOC}. We did not see any change in the I-V relation of I_{SOC} after partial inhibition by BoNT A, so we could find no evidence that SNAP-25 modifies the conductance properties of the Ca^{2+} entry channels in the way that syntaxin modulates the gating of voltage-activated Ca^{2+} channels (Bezprozvanny et al., 1995). Instead, loss of functional SNAP-25 simply reduces the amplitude of the residual I_{SOC}.

Conclusions regarding the Mechanism of Coupling

Ca^{2+} entry into oocytes can be activated by microinjection of extracts from lymphocytes or yeast in which Ca^{2+} stores have been pharmacologically or genetically depleted (Csutora et al., 1999). However, those authors acknowledged that oocytes themselves produce relatively low levels of calcium influx factor, and that the evoked influx had different properties from endogenously stimulated capacitative Ca^{2+} entry, especially in lanthanide sensitivity. Our present results come entirely from oocytes and do not rule out the potential importance of diffusible factors in other cell types. A conformational coupling hypothesis could be compatible with our data if one assumes that the link between the stores and the plasma membrane is mechanically weak before store depletion and strong afterward, and that SNAP-25 or a homolog is important for the linkage. Our results are somewhat more naturally accommodated within a model in which the channels themselves or membrane-bound activator molecules are exocytotically incorporated into the plasma membrane upon store depletion. We would argue that inhibitions by BoNT A and dominant-negative SNAP-25 are far more likely to be pharmacologically specific for SNAP-25 and exocytosis than the previous controversial effects of GTPγS, primaquine, and cytoskeletal inhibitors. Furthermore, new experiments with cytoskeletal modulation have provided fresh evidence for secretion-like coupling (Patterson et al., 1999). The major arguments against exocytosis are the lack of measurable increases in membrane capacitance before or during store-operated Ca^{2+} entry in oocytes (<1% change; preliminary data of Y. Y.) and other cell types (e.g., Fomina and Nowycky, 1999), and the lack of effect of BoNT B and E and tetanus toxin. However, the negligible capacitance increases could reflect the minuscule amount of membrane required to accommodate the channels or activators, swamped by the huge amount of concurrent exo- and endocytosis, sufficient to replace the entire oocyte plasma membrane once every day if all components mixed freely (Zampighi et al., 1999). The lack of inhibition by certain toxins might be due to imperfect homology of the relevant oocyte components to the better-studied mammalian SNAREs; we had no positive control that our toxin samples had any effect in oocytes. Nevertheless, the involvement of proteins extensively studied in exocytosis opens up many possible testable hypotheses and experiments for the future.

Experimental Procedures

Cell Preparation and Electrophysiology

Oocytes were cultured in Barth's medium supplemented with 5% horse serum to increase viability of the cells (Quick et al., 1992). Recordings were taken at least 2 hr after removal of the serum. Oocytes used to assess drug action were obtained from the same frog to reduce variability in I_{SOC}. Extracellular solution compositions and recording of whole-oocyte membrane currents with a conventional two-electrode voltage clamp were as described by Yao and Tsien (1997). Membrane potential was held at −60 mV unless otherwise specified. Capacitance of whole-oocyte plasma membrane was determined by $C_m = \int i_C\, dt/\Delta V$, where C_m is membrane capacitance, i_C capacitance current transient, ΔV membrane voltage step. C_m was averaged from ΔV of 5, 10, and 15 mV, respectively.

Giant-patch glass pipettes (#7052, O. D./I. D. 1.65/1.1, WPI, FL or borosilicate glass, O. D./I. D. 1.5/0.86 Warner Instrument Corp., Hamden, CT) were pulled to have tip openings of around 40 μm with a horizontal electrode puller (P-80/PC, Sutter Instrument Co., Novato, CA). The pipette tips were then heat-polished to give final openings of about 30 μm, which should encompass about 1/6400 of the total surface of an oocyte of 1.2 mm diameter. Thus, an oocyte with a total I_{SOC} of 100 nA should give about 16 pA through the patch assuming the channels are evenly distributed. Patch recordings made from various sites on the animal hemisphere showed no significant variation in current amplitudes. In some experiments (e.g., Figure 1), $I_{Cl,Ca}$ was measured as a more sensitive monitor of Ca^{2+} influx, because its amplitude is about an order of magnitude larger than I_{SOC} (Yao and Tsien, 1997). For intrapipette perfusion, quartz capillaries (O. D./I. D. 150/75 μm, Polymicro Technologies Inc., Phoenix, AZ) were pulled and the tips cut to about 15 to 20 μm diameter. Two capillaries were bundled with glue and inserted to within 100–200 μm of the patch pipette tip under a stereo microscope. Perfusates were passed through a 2 μm filter. Perfusates in quartz capillaries were held by suction (typically −10 mm Hg) to prevent leakage and were ejected by a positive pressure (typically 150 mm Hg). Turnover of intrapipette solutions at the membrane was typically within a few seconds. Oocyte vitelline membranes were removed in a hyperosmotic solution that contained (mM): KCl 200, $MgCl_2$ 2, KCl 1, and HEPES 5, titrated to pH 7.2 with NaOH, supplemented with EGTA 5 mM for measuring I_{SOC} or 40 μM for measuring $I_{Cl,Ca}$. Current was recorded with an Axopatch 200B amplifier (Axon Instruments, Inc., Foster City, CA), whose range of the fast capacitance compensation was expanded to 20 pF by the manufacturer. Membrane seal resistance were larger than 1 GΩ. Bath solution for excised patch recordings was a mock intracellular Ringer (IR), containing (mM): 95 KCl, 1 NaCl, 5 $MgCl_2$, 5 HEPES, titrated to pH 7.2 with NaOH, plus EGTA 5 mM and 40 μM, respectively, for recording I_{SOC} and $I_{Cl,Ca}$. Membrane potentials of the oocytes were measured to be −8.8 ± 0.5 mV (n = 4) in IR. The pipette potential was held at 50 mV after a GΩ seal was formed. A voltage ramp command from 50 to −130 mV with a duration of 0.5 s was repetitively applied at 30 s intervals to allow rapid collection of I-V relations of the current. This resulted in a final membrane potential ramp from −109 to 71 mV after summing pipette holding potential, oocyte membrane potential, and the ramp command.

All recordings were performed at room temperature (22°C ± 2°C). Data points are expressed as mean ± SE. Statistical significance of drug actions was evaluated with two-tailed Student's t test using Origin software (Microcal, Northampton, MA).

Use of TPEN to Activate Store-Operated Ca^{2+} Influx in *Xenopus* Oocytes

The usual means for dumping Ca^{2+} stores and activating I_{SOC}, such as ionomycin administration or metabolic production or microinjection of $InsP_3$, were poorly reversible. A rapidly reversible agent not requiring microinjection would be very helpful. A membrane-permeant chelator of divalent cations, TPEN, was shown recently to induce store-operated Ca^{2+} influx in mammalian cells (Hofer et al., 1998). TPEN has a low affinity for Ca^{2+} (K_D = 40 μM; Arslan et al., 1985) suitable for buffering the relatively high free Ca^{2+} concentrations in the lumen of Ca^{2+}-accumulating organelles while exerting little effect on cytosolic free Ca^{2+} (Hofer et al., 1998). The total Ca^{2+} inside the stores is conserved during application of TPEN because the TPEN–Ca^{2+} complex is impermeant (Arslan et al., 1985). When free extracellular TPEN is removed, the intraluminal TPEN–Ca^{2+} dissociates and rapidly restores intraluminal free Ca^{2+} so that deactivation of influx can be studied.

TPEN had not been previously tested in *Xenopus* oocytes but proved very useful in activating I_{SOC} because of the above advantages. TPEN was dispersed in nominally Ca^{2+}-free media and applied extracellularly to load the oocytes before restoration of normal Ca^{2+} to measure the influx. The minimum TPEN concentrations required to activate the Ca^{2+} influx varied from 0.1 to 1 mM in different batches of oocytes. Ca^{2+} influx reversed quickly after washout of TPEN from bath and could be reactivated repeatedly. Maximal Ca^{2+} influx was activated by preincubation of oocyte with TPEN for 1 min. Longer incubations with TPEN slowed the deactivation time course of the Ca^{2+} influx. An additional inward nonspecific current was present during the TPEN loading, which was not inhibited by injection of EGTA. To test whether the action of TPEN was additive to that of ionomycin, Ca^{2+} influx was first induced by TPEN and then ionomycin to obtain their individual activities in the same oocyte. Ca^{2+} influx induced by ionomycin was long-lasting. Application of TPEN after ionomycin did not induce additional Ca^{2+} influx (data not shown). Such occlusion indicates that Ca^{2+} influx induced by TPEN is through the store-operated Ca^{2+} influx pathway.

One concern with TPEN is its very high binding affinity for Zn^{2+} ($K_D = 2.63 \times 10^{-16}$ M) (Arslan et al., 1985). Also, even 5 mM TPEN only activated I_{SOC} to about half the maximal amplitude obtainable with other means for depleting stores. A new membrane-permeable Ca^{2+} chelator that has a higher affinity to Ca^{2+} and lower affinity to Zn^{2+} than TPEN would be yet better. Fortunately, inhibition of BoNTs by TPEN's chelation of Zn^{2+} is irrelevant because TPEN is only applied well after BoNT injection.

Materials

Botulinum toxin A, B, and E were kindly supplied by Dr. B. R. DasGupta (University of Wisconsin, Madison). They were dissolved at 1 mg/ml in buffer containing (mM): 150 NaCl, 10 HEPES, titrated to pH 7.0, maintained at −80°C. BoNTs were reduced with 10 or 20 mM DTT at room temperature for 1 hr before injection. Activity of BoNT A was assessed by in vitro cleavage assay of SNAP-25 (Ferrer-Montiel et al., 1996). Cytochalasin D was from Sigma. C3 transferase, amiloride, and brefeldin A were from Calbiochem Novabiochem (La Jolla, CA). One side effect of C3 transferase was a spontaneous current, dependent on extracellular Ca^{2+}, which usually developed about 1 hr or longer after the injection of C3. Intracellular injection of EGTA or exposure to TPEN suppressed the current, so it did not interfere with measurement of I_{SOC}. The origin of this curious current remained to be further characterized.

Expression Vector Construction and In Vitro Transcription

cDNAs of wild-type Rho A, its constitutively active mutant 63L, and dominant-negative mutant 19N in plasmid pCMV5 were kind gifts of Dr. G. Bokoch (Scripps Research Institute, San Diego, CA). Rho and its mutant cDNA inserts were released from pCMV5 with HindIII digestion and subcloned into pSGEM at the HindIII site. Vector pSGEM was obtained from Dr. Philipp and Dr. Flockerzi (Universität des Saarlandes, Homburg/Saar, Germany), which derived from a popular oocyte expression vector pGEMHE that contained *Xenopus* β-hemoglobin untranslated regions flanking the multiple cloning site (Liman et al., 1992). The orientation of the cDNA inserts was checked by gel electrophoresis after EcoRV digestion.

C-terminal truncated mutants of mouse SNAP-25 were created by PCR using a forward primer paired with various reverse primers that introduced a stop codon to terminate translation at different C-terminal sites of SNAP-25. The forward primer in PCR reaction had the sequence 5′-CGGGATCCGCCACCATGGCCGAGGACGCA GACATG, which contained a BamHI site and a Kozak sequence at the 5′ end of SNAP-25. The reverse primers for CΔ9, CΔ11, CΔ14, CΔ17, CΔ20, and CΔ41 were, respectively, 5′-CGGAATTCTTATTGG TTGGCTTCATCAAT, 5′-CGGAATTCTTAGGCTTCATCAATTCTGGT, 5′-CGGAATTCTTAAATTCTGGTTTTGTTGGA, 5′-CGGAATTCTTATT TGTTGGAGTCAGCCTT, 5′-CGGAATTCTTAGTCAGCCTTCTCCAT GAT, and 5′-CGGAATTCTTATAGGGCCATATGACGGAG. All reverse primers incorporated an EcoRI site and a stop codon at the 3′-end of SNAP-25. Following PCR amplification, the PCR products were gel-separated and digested with BamHI and EcoRI. The resulting PCR frgments were subcloned into the vector pSGEM between the 5′ UTR and the 3′UTR of *Xenopus* β-globin. All C-terminal truncation mutants of SNAP-25 were verified by DNA sequencing.

cDNAs of three subunits of epithelial sodium channel, α, β, γ, in plasmids pSPORT (α and γ) and pSD5 (β), were kind gifts of Dr. C. Canessa (Yale University). pSPORT-α and γ were linearized by NotI and RNA synthesized by T7 polymerase, whereas BglII and SP6 polymerase were used for pSD5-β. A mixture of the three cRNAs (0.1 or 1 ng each) was injected into each oocyte, and I_{ENaC} was measured 1–3 days later.

Capped cRNAs were synthesized using mMESSAGE mMACHINE kits from Ambion (Austin, TX). Synthetic cRNAs were resuspended in water. Aliquots of 2 μl each were stored at −80°C until injection. Typically, 20 nl RNA solution was injected into each oocyte. Concentrations of RNA were adjusted to reach the final desired mass.

Acknowledgments

We thank Dr. J. Llopis and Dr. J. Garcia-Sancho for their unpublished data and discussion, Dr. D. Hilgemann and Dr. C. C. Lu for discussion of the giant-patch recording technique, and Ms. Q. Xiong for technical assistance. This study was supported by grants to R. Y. T. from the Human Frontier Science Program (RG520/1995-M), National Institutes of Health (NS27177), and Howard Hughes Medical Institute, and a Department of the Army Medical Research Grant DAMD17-C-98-C-8040 to M. M.

Received June 8, 1999; revised July 21, 1999.

References

Allbritton, N.L., Meyer, T., and Stryer, L. (1992). Range of messenger action of calcium ion and inositol 1,4,5-trisphosphate. Science *258*, 1812–1815.

Arslan, P., Di Virgilio, F., Beltrame, M., Tsien, R.Y., and Pozzan, T. (1985). Cytosolic Ca^{2+} homeostasis in Ehrlich and Yoshida carcinomas. A new, membrane-permeant chelator of heavy metals reveals that these ascites tumor cell lines have normal cytosolic free Ca^{2+}. J. Biol. Chem. *260*, 2719–2727.

Barish, M.E. (1983). A transient calcium-dependent chloride current in the immature *Xenopus* oocytes. J. Physiol. (Lond.). *342*, 309–325.

Berridge, M.J. (1995). Capacitative calcium entry. Biochem. J. *312*, 1–11.

Bezprozvanny, I., Scheller, R.H., and Tsien, R.W. (1995). Functional impact of syntaxin on gating of N-type and Q-type calcium channels. Nature *378*, 623–626.

Bird, G.S., and Putney, J.W., Jr. (1993). Inhibition of thapsigargin-induced calcium entry by microinjected guanine nucleotide analogues. Evidence for the involvement of a small G protein in capacitative Ca^{2+} entry. J. Biol. Chem. *268*, 21486–21488.

Calakos, N., and Scheller, R.H. (1996). Synaptic vesicle biogenesis, docking, and fusion: a molecular description. Physiol. Rev. *76*, 1–29.

Cheatham, B., Volchuk, A., Kahn, C.R., Wang, L., Rhodes, C.J., and Klip, A. (1996). Insulin-stimulated translocation of GLUT4 glucose transporters requires SNARE-complex proteins. Proc. Natl. Acad. Sci. USA *93*, 15169–15173.

Chen, F., Foran, P., Shone, C.C., Foster, K.A., Melling, J., and Dolly, J.O. (1997). Botulinum neurotoxin B inhibits insulin-stimulated glucose uptake into 3T3-L1 adipocytes and cleaves cellubrevin unlike type A toxin which failed to proteolyze the SNAP-23 present. Biochemistry *36*, 5719–5728.

Csutora, P., Su, Z., Kim, H.K., Bugrim, A., Cunningham, K.W., Nuccitelli, R., Keizer, J.E., Hanley, M.R., Blalock, J.E., and Marchase, R.B. (1999). Calcium influx factor is synthesized by yeast and mammalian cells depleted of organellar calcium stores. Proc. Natl. Acad. Sci. USA *96*, 121–126.

Fasolato, C., Hoth, M., and Penner, R. (1993). A GTP-dependent step in the activation mechanism of capacitative Ca^{2+} influx. J. Biol. Chem. *268*, 20737–20740.

Favre, C.J., Nusse, O., Lew, D.P., and Krause, K.H. (1996). Store-operated Ca^{2+} influx: what is the message from the stores to the membrane? J. Lab. Clin. Med. *128*, 19–26.

Ferrer-Montiel, A.V., Canaves, J.M., DasGupta, B.R., Wilson, M.C., and Montal, M. (1996). Tyrosine phosphorylation modulates the activity of clostridial neurotoxins. J. Biol. Chem. *271*, 18322–18325.

Ferrer-Montiel, A.V., Gutierrez, L.M., Apland, J.P., Canaves, J.M., Gil, A., Viniegra, S., Biser, J.A., Adler, M., and Montal, M. (1998). The 26-mer peptide released from SNAP-25 cleavage by botulinum neurotoxin E inhibits vesicle docking. FEBS Lett. *435*, 84–88.

Fomina, A.F., and Nowycky, M.C. (1999). A current activated on depletion of intracellular Ca^{2+} stores can regulate exocytosis in adrenal chromaffin cells. J. Neurosci. *19*, 3711–3722.

Gregory, R.B., and Barritt, G.J. (1996). Store-activated Ca^{2+} inflow in *Xenopus laevis* oocytes: inhibition by primaquine and evaluation of the role of membrane fusion. Biochem. J. *319*, 755–760.

Gutierrez, L.M., Canaves, J.M., Ferrer-Montiel, A.V., Reig, J.A., Montal, M., and Viniegra, S. (1995). A peptide that mimics the carboxy-terminal domain of SNAP-25 blocks Ca^{2+}-dependent exocytosis in chromaffin cells. FEBS Lett. *372*, 39–43.

Hall, A. (1998). Rho GTPases and the actin cytoskeleton. Science *279*, 509–514.

Hartzell, H.C. (1996). Activation of different Cl currents in *Xenopus* oocytes by Ca liberated from stores and by capacitative Ca influx. J. Gen. Physiol. *108*, 157–175.

Hilgemann, D.W. (1995). The giant membrane patch. In Single-Channel Recording (2nd edition), B. Sakmann and E. Neher, eds. (New York: Plenum Press), pp. 307–327.

Hofer, A.M., Fasolato, C., and Pozzan, T. (1998). Capacitative Ca^{2+} entry is closely linked to the filling state of internal Ca^{2+} stores: a study using simultaneous measurements of I_{CRAC} and intraluminal $[Ca^{2+}]$. J. Cell Biol. *140*, 325–334.

Holda, J.R., and Blatter, L.A. (1997). Capacitative Ca^{2+} entry is inhibited in vascular endothelial cells by disruption of cytoskeletal microfilaments. FEBS Lett. *403*, 191–196.

Holda, J.R., Klishin, A., Sedova, M., Huser, J., and Blatter, L.A. (1998). Capacitative calcium entry. News Physiol. Sci. *13*, 157–163.

Huang, X., Wheeler, M.B., Kang, Y.-h., Sheu, L., Lukacs, G.L., Trimble, W.S., and Gaisano, H.Y. (1998). Truncated SNAP-25 (1–197), like botulinum neurotoxin A, can inhibit insulin secretion from HIT-T15 insulinoma cells. Mol. Endocrinol. *12*, 1060–1070.

Jaconi, M., Pyle, J., Bortolon, R., Ou, J., and Clapham, D. (1997). Calcium release and influx colocalize to the endoplasmic reticulum. Curr. Biol. *7*, 599–602.

Kramer, R.H. (1990). Patch cramming: monitoring intracellular messengers in intact cells with membrane patches containing detector ion channels. Neuron *4*, 335–341.

Lewis, R.S., and Cahalan, M.D. (1995). Potassium and calcium channels in lymphocytes. Annu. Rev. Immunol. *13*, 623–653.

Liman, E.R., Tytgat, J., and Hess, P. (1992). Subunit stoichiometry of a mammalian K+ channel determined by construction of multimeric cDNAs. Neuron *9*, 861–871.

Montecucco, C., and Schiavo, G. (1995). Structure and function of tetanus and botulinum neurotoxins. Quart. Rev. Biophys. *28*, 423–472.

Parekh, A.B., and Penner, R. (1997). Store depletion and calcium influx. Physiol. Rev. *77*, 901–930.

Parekh, A.B., Terlau, H., and Stühmer, W. (1993). Depletion of $InsP_3$ stores activates a Ca^{2+} and K^+ current by means of a phosphatase and a diffusible messenger. Nature *364*, 814–818.

Parker, I., and Ivorra, I. (1993). Confocal microfluorimetry of calcium signals evoked in *Xenopus* oocytes by photoreleased inositol trisphosphate. J. Physiol. *461*, 133–165.

Patterson, R.L., van Rossum, D.B., and Gill, D.L. (1999). Store-operated Ca^{2+} entry: evidence for a secretion-like coupling model. Cell *98*, this issue, 487–499.

Petersen, C.C.H., and Berridge, M.J. (1995). G-protein regulation of capacitative Ca^{2+} entry may be mediated by protein kinases A and C in *Xenopus* oocytes. Biochem. J. *307*, 663–668.

Petersen, C.C.H., and Berridge, M.J. (1996). Capacitative calcium entry is colocalised with calcium release in *Xenopus* oocytes: evidence against a highly diffusible calcium influx factor. Pflug. Arch. Eu. J. Physiol. *432*, 286–292.

Peyroche, A., Antonny, B., Robineau, S., Acker, J., Cherfils, J., and Jackson, C.L. (1999). Brefeldin A acts to stabilize an abortive ARF-GDP-Sec7 domain protein complex: involvement of specific residues of the Sec7 domain. Mol. Cell *3*, 275–285.

Putney, J.W., Jr., and McKay, R.R. (1999). Capacitative calcium entry channels. BioEssays *21*, 38–46.

Quick, M.W., Naeve, J., Davidson, N., and Lester, H.A. (1992). Incubation with horse serum increases viability and decreases background neurotransmitter uptake in *Xenopus* oocytes. Biotechniques *13*, 357–361.

Randriamampita, C., and Tsien, R.Y. (1993). Emptying of intracellular Ca^{2+} stores releases a novel small messenger that stimulates Ca^{2+} influx. Nature *364*, 809–814.

Ribeiro, C.M.P., Reece, J., and Putney, J.W., Jr. (1997). Role of the cytoskeleton in calcium signaling in NIH 3T3 cells: an intact cytoskeleton is required for agonist-induced $[Ca^{2+}]_i$ signaling, but not for capacitative calcium entry. J. Biol. Chem. *272*, 26555–26561.

Rossetto, O., Schiavo, G., Montecucco, C., Poulain, B., Deloye, F., Lozzi, L., and Shone, C.C. (1994). SNARE motif and neurotoxins. Nature *372*, 415–416.

Rossi, G., Salminen, A., Rice, L.M., Brünger, A.T., and Brennwald, P. (1997). Analysis of a yeast SNARE complex reveals remarkable similarity to the neuronal SNARE complex and a novel function for the C terminus of the SNAP-25 homolog, Sec9. J. Biol. Chem. *272*, 16610–16617.

Schmalzing, G., Richter, H.P., Hansen, A., Schwarz, W., Just, I., and Aktories, K., (1995). Involvement of the GTP binding protein Rho in constitutive endocytosis in *Xenopus laevis* oocytes. J. Cell Biol. *130*, 1319–1332.

Shimkets, R.A., Lifton, R.P., and Canessa, C.M. (1997). The activity of the epithelial sodium channel is regulated by clathrin-mediated endocytosis. J. Biol. Chem. *272*, 25537–25541.

Shurety, W., Stewart, N.L., and Stow, J.L. (1998). Fluid-phase markers in the basolateral endocytic pathway accumulate in response to the actin assembly-promoting drug jasplakinolide. Mol. Biol. Cell *9*, 957–975.

Sokabe, M., and Sachs, F. (1990). The structure and dynamics of patch-clamped membranes: a study using differential interference contrast light microscopy. J. Cell Biol. *111*, 599–606.

Solsona, C., Innocenti, B., and Fernandez, J.M. (1998). Regulation of exocytotic fusion by cell inflation. Biophys. J. *74*, 1061–1073.

Somasundaram, B., Norman, J.C., and Mahaut-Smith, M.P. (1995). Primaquine, an inhibitor of vesicular transport, blocks the calcium-release-activated current in rat megakaryocytes. Biochem. J. *309*, 725–729.

Sutton, R.B., Fasshauer, D., Jahn, R., and Brunger, A.T. (1998). Crystal structure of a SNARE complex involved in synaptic exocytosis at 2.4 Å resolution. Nature *395*, 347–353.

Tamori, Y., Hashiramoto, M., Araki, S., Kamata, Y., Takahashi, M., Kozaki, S, and Kasuga, M. (1996). Cleavage of vesicle-associated membrane protein (VAMP)-2 and cellubrevin on GLUT4-containing vesicles inhibits the translocation of GLUT4 in 3T3-L1 adipocytes. Biochem. Biophys. Res. Commun. *220*, 740–745.

Van Aelst, L., and D'Souza-Schorey, C. (1997). Rho GTPases and signaling networks. Genes Dev. *11*, 2295–2322.

Van den Berghe, N., Barros, L.F., van Mackelenbergh, M.G., and Krans, H.M. (1996). *Clostridium botulinum* C3 exoenzyme stimulates GLUT4-mediated glucose transport, but not glycogen synthesis, in 3T3-L1 adipocytes—a potential role of rho? Biochem. Biophys. Res. Commun. *229*, 430–439.

Weimbs, T., Mostov, K.E., Lows, S.H., and Hofmann, K. (1998). A model for structural similarity between different SNARE complexes based on sequence relationships. Trends Cell Biol. *8*, 260–262.

Xu, T., Binz, T., Niemann, H., and Neher, E. (1998). Multiple kinetic components of exocytosis distinguished by neurotoxin sensitivity. Nat. Neurosci. *1*, 192–200.

Yao, Y., and Tsien, R.Y. (1997). Calcium current activated by depletion of calcium stores in *Xenopus* oocytes. J. Gen. Physiol. *109*, 703–715.

Yao, Y., Choi, J., and Parker, I. (1995). Quantal puffs of intracellular Ca^{2+} evoked by inositol trisphosphate in *Xenopus* oocytes. J. Physiol. *482*, 533–553.

Zampighi, G.A., Loo, D.D.F., Kreman, M., Eskandari, S., and Wright, E.M. (1999). Functional and morphological correlates of connexin50 expressed in *Xenopus laevis* oocytes. J. Gen. Physiol. *113*, 507–523.